Reduced Coercive Field in $BiFeO_3$ Thin Films Through Domain Engineering

Vilas Shelke, Dipanjan Mazumdar, Gopalan Srinivasan, Amit Kumar, Stephen Jesse, Sergei Kalinin, Arthur Baddorf, and Arunava Gupta**

The bismuth ferrite ($BiFeO_3$) material offers a comprehensive package of multifunctionality. In addition to the multiferroic behavior, i.e., coexistence of electric and magnetic orderings,[1] it also exhibits a photovoltaic effect,[2] metal-insulator transition,[3] electric modulation of conduction,[4] and terahertz radiation emission.[5] The lead-free composition and above room temperature multifunctionality make $BiFeO_3$ a potential material for a wide variety of applications in terms of sensors, memories, and spintronic devices.[6] The high value of ferroelectric polarization is very promising for next-generation ferroelectric random-access memory devices. However, the high value of the coercive field is a major hurdle for the fabrication of practical devices. Here, we report an easy-to-perform domain engineering approach to reduce the coercive field significantly in $BiFeO_3$ thin films.

In general, three fundamental parameters, viz. polarization, leakage current, and applied electric field encompass the domain of ferroelectric applications. A wider domain, as shown schematically in **Figure 1**a, is always desired with a higher value of remnant polarization (P_r), inverse leakage current (J_c^{-1}), and inverse coercive field (E_c^{-1}). Significantly higher values of remnant polarization have been reported in $BiFeO_3$ thin films through use of lattice matched, vicinal, and different orientation substrates.[7–10] Similarly, the leakage current mechanism at macroscopic[11–14] and microscopic[15] scales have been studied with the intention of achieving reduced values. Comparatively, success in achieving lower values of the coercive field has so far been limited. Most of the reports on films with "enhanced" polarization and "reduced" leakage current have coercive fields of around 200 kV cm^{-1}. The immediate consequence of such a high switching field is the decomposition of $BiFeO_3$ into magnetite (Fe_3O_4) and bismuth oxide (Bi_2O_3) compounds.[16] The higher value of E_c may exceed the breakdown voltage disqualifying the material as a genuine ferroelectric.[17] It also affects the operational parameters like switching time and fatigue. Recently, Kim et al. reported an empirical dependence of the coercive field on the thickness (d) of BFO films, in accordance with the Kay-Dunn scaling law $E_c \propto d^{(-2/3)}$.[18] Still, the value of the coercive field for 960-nm thick BFO film was quite high. The lowest value of coercive field to date has been reported by Jang et al. in a strain-free $BiFeO_3$ membrane.[19,20] The state of the art process of $BiFeO_3$ membrane formation yielded an E_c value of 80 kV cm^{-1} in a 600-nm thick membrane. On the other hand, high-quality single crystals exhibit coercive field as low as 12 kV cm^{-1}.[21] Thus, the unavailability of straightforward means to achieve a lower value of coercive field can hamper the prospects of ferroelectric and multiferroic applications of $BiFeO_3$ thin films.

The films deposited on $SrTiO_3$ (100), (110), and (111) substrates have four, two and one polarization variants, respectively.[22] Similarly, the STO substrate with 4^0 miscut along [100] direction reduces the number of variants to two, resulting in stripe domains.[10] The reduction of polarization variants has profound effect on the polarization value, which reaches above 100 μC cm^{-2} for single variant or monodomain films. However, the switchability does not improve with the reduction in number of variants and consequently the coercive field remains very high.[23] On the contrary, theoretical study suggests that the structural inhomogeneities can reduce the energy barrier for the domain nucleation during polarization switching and the coercive field can decrease as the number of variants increases.[24] An intermediate dictum can be followed by breaking the symmetry of ferroelectric variants through appropriately directed vicinal substrates. A schematic diagram of (100) vicinal substrate with 4^0 miscut along [100] and [110] is illustrated in Figure 1b. For the 4^0 miscut along [100] direction, the substrate has parallel step pattern with terrace width of around 15.8 nm.[25] The films deposited on such surface mimics the crystal facets stripe domain structure with two variants.[10] On the other hand, the surface with miscut along [110] direction has a saw-tooth step pattern with a terrace width of 28.3 nm. Such surfaces can effectively impart the necessary tilt and break in the symmetry of polarization variants. The domain structure of these films will be different than that deposited on plain (110) oriented substrates.

We deposited $BiFeO_3$ thin films with a $SrRuO_3$ bottom electrode on plain STO (100), STO (100) with 4^0 miscut along [100], STO (100) with 4^0 miscut along [110] and plain STO (110) substrates. The variation of ferroelectric polarization (P) with applied voltage (V) for 320 nm BFO films is shown in

Dr. V. Shelke, Dr. D. Mazumdar, Prof. A. Gupta
Center for Materials for Information Technology
University of Alabama
Tuscaloosa, Alabama 35487 – 0209, USA
E-mail: agupta@mint.ua.edu; drshelke@gmail.com
Prof. G. Srinivasan
Physics Department
Oakland University
Rochester, Michigan 49309 – 4401, USA
A. Kumar, Dr. S. Jesse, Dr. S. Kalinin, Dr. A. Baddorf
Center for Nanophase Materials Science
Oak Ridge National Laboratory
Oak Ridge, TN 37831, USA

DOI: 10.1002/adma.201000807

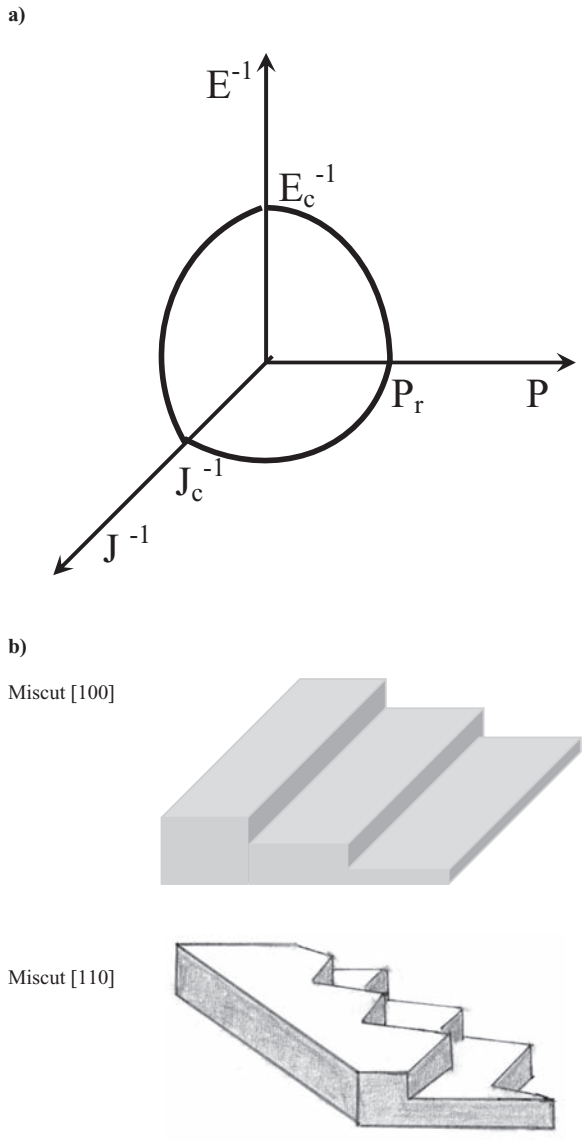

Figure 1. a) A Schematic presentation of the domain of ferroelectric applications encompassed by three fundamental parameters viz polarization, leakage current and electric field; b) A schematic diagram of the substrate terrace with miscut along [100] and [110] directions.

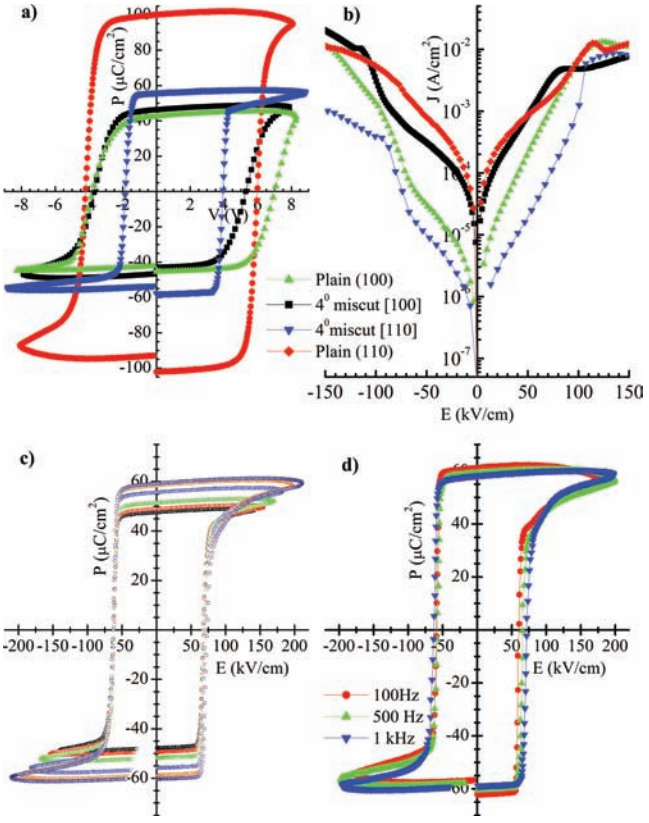

Figure 2. a) Ferroelectric polarization of 320 nm BFO films on different substrates; b) Leakage current behavior of 320 nm BFO films on different substrates and c)Field dependant variation, d) frequency dependant variation of ferroelectric polarization of 640 nm BFO film on STO 4^0 miscut [110] substrate.

Figure 2a. The BFO film on plain STO (100) substrate shows low remnant polarization (P_r) value (45 μC cm^{-2}) and high switching voltage. A slight improvement in polarization value and reduction in switching voltage is seen in the films deposited on STO (100) substrate with 4^0 miscut along [100] direction.[10] The ferroelectric behavior is even better when the substrate miscut is along [110] direction. This film has remnant polarization 58 μC cm^{-2} and the switching is accomplished with voltage less than 4 V. Such low voltage is primary requisite for the electronics applications of ferroelectric materials. The BFO film on STO (110) substrate shows a very high polarization value (P_r ~ 100 μC cm^{-2}). However, the voltage required for the switching is also higher as compared to the films on miscut substrate. The leakage current behavior of 320 nm films on different substrates is shown in Figure 2b. At higher field, there is no significant difference in the leakage current values. In the low field regime, the leakage current is lower for the films on [110] miscut substrate. The reduced value of leakage current can assist the effective switching so that the coercive field remains smaller than the breakdown field.[17] However, this may not be the only reason for the low value of coercive bias in these films. In order to lower the coercive bias, defects are needed which can act as nucleation sites. However, structural defects also act as center for materials decomposition and leakage paths. The BFO film deposited on miscut substrate with saw-tooth steps is constrained. The nucleation sites in this case are defined by the tilt and are not associated with the discontinuities in the crystallographic lattice. It results in creation of population of good and non-leaky defects. Therefore, the coercive bias is lowered without increase in the leakage current.

In order to reduce the switching field further, we deposited 640 nm BFO film on the substrate with 4^0 miscut along [110]. The electric field dependence of polarization for the 640 nm film is shown in Figure 2c. The conventional ferroelectrics show gradual increase in polarization value as the applied field is increased. The polarization behavior of BFO is slightly different in terms of remnant polarization, which is quite close to the saturation value. The macroscopic switching behavior is the collective effect of domain nucleation and domain wall motion. The [110] vicinal substrate used by us can provide

excessive nucleation sites through the saw-tooth step patterns. Therefore, a remnant polarization of 60 μC cm^{-2} and a significantly lower coercive field (74 kV cm^{-1}) is seen in this sample. To the best of our knowledge, the E_c = 74 kV cm^{-1} is the lowest reported value for BFO thin films. Previously, Jang et al. reported E_c = 80 kV cm^{-1} in 400- and 600-nm thick strain-free membrane detached from the wafer.[19,20] The improvement of ferroelectric behavior in BFO membrane is considered due to reduced leakage current and easy domain wall motion arising from the freedom of substrate clamping. They also reported a polarization value of 102 μC cm^{-2} and a coercive field of 200 kV cm^{-1} for (111)-oriented BFO film. The higher value of coercive field was attributed to the substrate clamping effect. Comparatively, our films are deposited through a simple procedure without the complication of lithography, etching, lift-off, etc. for the membrane formation.[19] The films are clamped to the substrate but are expected to be strain-relaxed with 640 nm thickness. The ferroelectric behavior remains almost invariant for various frequencies in the range 100 Hz – 1 kHz as shown in Figure 2d. It is noteworthy that a high frequency measurement is sometimes preferred to mitigate the effect of leakage and thus obtain better polarization characteristics. For similar reason, low-temperature measurement is also used.[26] The low coercive field and reasonably high polarization value for our sample is obtained at room temperature and over a wide frequency range. Therefore, this approach can be quite suitable for practical device applications.

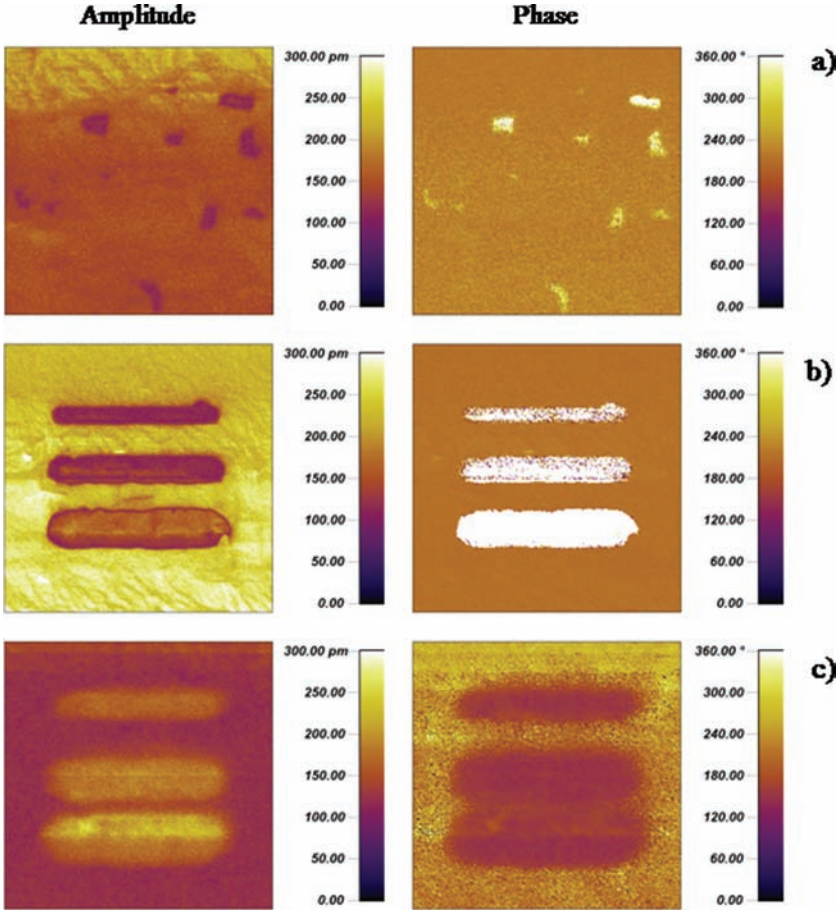

Figure 3. PFM images with amplitude and phase scans of a) as-grown BFO film on [110] vicinal substrate b) electrically "written" line patterns with +10, +15, and +20 V dc bias, and c) electrically 'written' line patterns with –10, –15, and –20 V dc bias (from top to bottom, respectively)

The piezo-response force microscopy (PFM) images of BFO film on miscut [110] substrate are shown in **Figure 3**a–c. The amplitude and phase scans in Figure 3a reveal the domain configuration of the as-grown film. The vicinal substrates are expected to control the architecture of domains through minimization of energy at step edges. The BFO films on 4^0 miscut [100] substrates have stripe domains with two variants resulting from the parallel terrace patterns of the substrates. On the other hand, irregular shaped fractal domains are observed in the films on plain STO substrate.[27] In our sample, miscut along [110] direction generates saw-tooth pattern of the terrace. As a result, further break in the symmetry of the domains is imparted with domains intermediate between stripe and fractal patterns. The electrically "written" line patterns with different positive and negative dc bias are shown in Figure 3b and 3c, respectively. The dc poling is clearly seen with ±10 V as compared to 12 V mentioned by Jang et al. for the BFO membrane.[19] It is noteworthy that due to the localized nature of the field distribution and ambient condition of the probe, a higher potential is required for the PFM switching than the macroscopic polarization measurement.

The ferroelectric switching is initiated in the neighborhood of the film/electrode interface. The switchability depends on the relative weakness of the bond formed between the film and electrode.[28] This fact remains invariant in the present case as the interfaces are always SRO–BFO at the bottom and BFO–Pt at the top. The thickness dependence of the coercive field in accordance with the Kay–Dunn law[18] can partially explain the reduction from E_c ~ 120 kV cm^{-1} in 320 nm film to 74 kV cm^{-1} in 640 nm BFO film on miscut [110] substrate. However, it does not account for the variation among the 320 nm films on different vicinal substrates. Qualitatively, it appears that the substrate with a miscut along the [110] direction stabilizes two-variant domains, thereby preserving an optimum polarization value. The saw-tooth terrace pattern breaks the domain symmetry and makes them more like fractal shape. In addition, it may also create step-edge dislocations, which can act as nucleation centers. Such domains with two-variants and extra nucleation sites may be easier to switch. As a result, the film exhibit lower value of coercive field and optimum value of polarization.

In summary, reduction of the coercive field is vital for the practical utility of BFO thin films. We have demonstrated that the coercive field can be reduced without affecting polarization

values through a domain engineering approach. The use of (100) substrate with 4^0 miscut along [110] direction, assists the growth of BFO films with 2-variants. However, the domains are intermediate between stripe and fractal geometry. The switching of such domains can be achieved with lower voltage. Such films exhibit the optimum polarization value (60 $\mu C\ cm^{-2}$) and reduced coercive field (74 $kV\ cm^{-1}$). Comparatively, the films on plain (100), miscut along [100] and plain (110) substrates have higher coercive field values.

Experimental Section

Thin films of $BiFeO_3$ (BFO) materials with thickness 320 and 640 nm were deposited using Pulsed Laser Deposition technique as reported elsewhere.[14] We used as-received single crystalline $SrTiO_3$ plain (100), (100) with 4^0 miscut along [100], (100) with 4^0 miscut along [110] and plain (110) oriented substrates. The BFO films were deposited sequentially with 50 nm $SrRuO_3$ (SRO) bottom layer and top "Pt" electrode of 250 μm diameter was sputter-deposited. The ferroelectric polarization and leakage current measurements were performed at room temperature using a ferroelectric tester (Premier II, Radiant Tech.). The domain structure was identified using Piezoresponse Force Microscope (Cypher, Asylum Research) for the as-deposited films. For the contrast imaging, positive and negative dc bias of 10–20 V was applied to the tip and subsequent scan with ac bias was done at 260 kHz.

Supporting Information

Supporting Information is available from the Wiley Online Library or from the author.

Acknowledgements

This work was supported by ONR under Grant No. N000 14 – 09-1 – 0119 and NSF NIRT under Grant No. CMS-0609377. A portion of this research was conducted at the Center for Nanophase Materials Sciences, which is sponsored at Oak Ridge National Laboratory by the Division of Scientific User Facilities, U.S. Department of Energy.

Received: March 5, 2010
Revised: August 1, 2010
Published online: December 7, 2010

[1] K. F.Wang, J. M.Liu, Z. F. Ren, *Adv. Phys.* **2009**, *58*, 32.
[2] T. Choi, S. Lee, Y. J. Choi, V. Kiryukhin, S. W. Cheong, *Science* **2009**, *324*, 63; b) S. Y. Yang, J. Seidel, S. J. Byrnes, P. Shafer, C.-H. Yang, M. D. Rossell, P. Yu, Y.-H. Chu, J. F. Scott, J.W. Ager, L. W. Martin, R. Ramesh, *Nat. Nanotechnol.* **2010**, *5*, 143.
[3] R Palai, R. S. Katiyar, H. Schmid, P. Tissot, S. J. Clark, J. Robertson, S. A. T. Redfern, G. Catalan, J. F. Scott, *Phys. Rev. B* **2008**, *77*, 014110.
[4] C. H. Yang, J. Seidel, S. Y. Kim, P. B. Rossen, P. Yu, M. Gajek, Y. H. Chu, L. W. Martin, M. B. Holcomb, Q. He, P. Maksymovych, N. Balke, S. V. Kalinin, A. P. Baddorf, S. R. Basu, M. L. Scullin, R. Ramesh, *Nat. Mater.* **2009**, *8*, 485.
[5] D. S. Rana, I. Kawayama, K. Mavani, K. Takahashi, H. Murakami, M. Tonouchi, *Adv. Mater.* **2009**, *21*, 2881.
[6] G. Catalan, J. F. Scott, *Adv. Mater.* **2009**, *21*, 2463.
[7] Y. H. Chu, Q. Zhan, L. W. Martin, M. P. Cruz, P. L. Yang, G. W. Pabst, F. Zavaliche, S. Y. Yang, J. X. Zhang, L. Q. Chen, D. G. Schlom, I. N. Lin, T. B. Wu, R. Ramesh, *Adv. Mater.* **2006**, *18*, 2307.
[8] J. Li, J. Wang, M. Wuttig, R. Ramesh, N. Wang, B. Ruette, A. P. Pyatakov, A. K. Zvezdin, D. Viehland, *Appl. Phys. Lett.* **2004**, *84*, 5261.
[9] R. R. Das, D. M. Kim, S. H. Baek, C. B. Eom, F. Zavaliche, S. Y. Yang, R. Ramesh, Y. B. Chen, X. Q. Pan, X. Ke, M. S. Rzchowski, S. K. Streiffer, *Appl. Phys. Lett.* **2006**, *88*, 242904.
[10] H. W. Jang, D. Ortiz, S. H. Baek, C. M. Folkman, R. R. Das, P. Shafer, Y. Chen, X. Pan, R. Ramesh, C. B. Eom, *Adv. Mater.* **2009**, *21*, 817.
[11] G. W. Pabst, L. W. Martin, Y. H. Chu, R. Ramesh, *Appl. Phys. Lett.* **2007**, *90*, 072902.
[12] L. Pintilie, C. Dragoi, Y. H. Chu, L. W. Martin, R. Ramesh, M. Alexe, *Appl. Phys. Lett.* **2009**, *94*, 232902.
[13] T. Kawae, Y. Terauchi, H. Tsuda, M. Kumeda, A. Morimoto, *Appl. Phys. Lett.* **2009**, *94*, 112904.
[14] V. Shelke, V. N. Harshan, S. Kotru, A. Gupta, *J. Appl. Phys.* **2009**, *106*, 104114.
[15] J. Seidel, L. W. Martin, Q. He, Q. Zhan, Y. H. Chu, A. Rother, M. E. Hawkridge, P. Maksymovych, P. Yu, M. Gajek, N. Balke, S. V. Kalinin, S. Gemming, F. Wang, G. Catalan, J. F. Scott, N. A. Spaldin, J. Orenstein, R. Ramesh, *Nat. Mater.* **2009**, *8*, 229.
[16] X. J. Lou, C. X. Yang, T. A. Tang, Y. Y. Lin, M.Zhang, J. F. Scott, *Appl. Phys. Lett.* **2007**, *90*, 262908.
[17] H. Bea, B. Dupe, S. Fusil, R. Mattana, E. Jacquet, B. Warot-Fonrose, F. Wilhelm, A. Rogalev, S. Petit, V. Cros, A. Anane, F. Petroff, K. Bouzehouane, G. Geneste, B. Dkhil, S. Lisenkov, I. Ponomareva, L. Bellaiche, M. Bibes, A. Barthelemy, *Phys. Rev. Lett.* **2009**, *102*, 217603.
[18] D. H. Kim, H. N. Lee, M. D. Biegalski, H. M. Christen, *Appl. Phys. Lett.* **2008**, *92*, 012911.
[19] H. W. Jang, S. H. Baek, D. Ortiz, C. M. Folkman, C. B. Eom, Y. H. Chu, P. Shafer, R. Ramesh, V. Vaithyanathan, D. G. Schlom, *Appl. Phys. Lett.* **2008**, *92*, 062910.
[20] H. W. Jang, S. H. Baek, D. Ortiz, C. M. Folkman, R. R. Das, Y. H. Chu, P. Shafer, J. X. Zhang, S. Choudhury, V. Vaithyanathan, Y. B. Chen, D. A. Felker, M. D. Biegalski, M. S. Rzchowski, X. Q. Pan, D. G. Schlom, L. Q. Chen, R. Ramesh, C. B. Eom, *Phys. Rev. Lett.* **2008**, *101*, 107602.
[21] D. Lebeugle, D. Colson, A. Forget, M. Viret, *Appl. Phys. Lett.* **2007**, *91*, 022907.
[22] Y. H. Chu, M. P. Cruz, C. H. Yang, L. W. Martin, P. L. Yang, J. X. Zhang, K. Lee, P. Yu, L. Q. Chen, R. Ramesh, *Adv. Mater.* **2007**, *19*, 2662.
[23] F. Zavaliche, S. Y. Yang, T. Zhao, Y. H. Chu, M. P. Cruz, C. B. Eom, R. Ramesh, *Phase Transition* **2006**, *79*, 991.
[24] S. Choudhury, L. Q. Chen, Y. L. Li, *Appl. Phys. Lett.* **2007**, *91*, 032902.
[25] G. B. Cho, M. Yamamoto, Y. Endo, *Thin Solid Films* **2004**, *464–465*, 80.
[26] J. H. Dho, X. D. Qi, H. Kim, J. L. MacManus-Driscoll, M. G. Blamire, *Adv. Mater.* **2006**, *18*, 1445.
[27] G. Catalan, H. Bea, S. Fusil, M. Bibes, P. Paruch, A. Barthelemy, J. F. Scott, *Phys. Rev. Lett.* **2008**, *100*, 027602.
[28] M. Stengel, D. Vanderbilt, N. A. Spaldin, *Nat. Mater.* **2009**, *8*, 392.